Accurate van der Waals coefficients between fullerenes and fullerene-alkali atoms and clusters: Modified single-frequency approximation

Jianmin Tao,[1,*] Yuxiang Mo,[1] Guocai Tian,[1,2] and Adrienn Ruzsinszky[1]

[1]*Department of Physics, Temple University, Philadelphia, Pennsylvania 19122-1801, USA*

[2]*State Key Laboratory of Complex Nonferrous Metal Resources Clean Utilization, Kunming University of Science and Technology, Kunming, Yunnan 650093, China*

(Received 29 April 2016; revised manuscript received 27 July 2016; published 15 August 2016)

Long-range van der Waals (vdW) interaction is critically important for intermolecular interactions in molecular complexes and solids. However, accurate modeling of vdW coefficients presents a great challenge for nanostructures, in particular for fullerene clusters, which have huge vdW coefficients but also display very strong nonadditivity. In this work, we calculate the coefficients between fullerenes, fullerene and sodium clusters, and fullerene and alkali atoms with the hollow-sphere model within the modified single-frequency approximation (MSFA). In the MSFA, we assume that the electron density is uniform in a molecule and that only valence electrons in the outmost *subshell* of atoms contribute. The input to the model is the static multipole polarizability, which provides a sharp cutoff for the plasmon contribution outside the effective vdW radius. We find that the model can generate C_6 in excellent agreement with expensive wave-function-based *ab initio* calculations, with a mean absolute relative error of only 3%, without suffering size-dependent error. We show that the nonadditivities of the coefficients C_6 between fullerenes and C_{60} and sodium clusters Na_n revealed by the model agree remarkably well with those based on the accurate reference values. The great flexibility, simplicity, and high accuracy make the model particularly suitable for the study of the nonadditivity of vdW coefficients between nanostructures, advancing the development of better vdW corrections to conventional density functional theory.

DOI: 10.1103/PhysRevB.94.085126

I. INTRODUCTION

Due to the high computational efficiency and useful accuracy, Kohn-Sham density functional theory (DFT) has reached a high level of sophistication and has become a standard electronic-structure theory [1,2]. In this theory, only the exchange-correlation energy component has to be approximated as a functional of the electron density. Most density functionals have been developed from the constraint satisfaction approach [3] or by fitting a designed functional form to a set of experiments or a combination of both. These conventionally developed density functionals can describe chemical bonds or short-range interactions [4] arising from the density overlap well for quantum chemistry [5–8] or condensed-matter physics [9,10] or both [11,12] but often fail to describe phenomena due to the long-range van der Waals interaction, such as physisorption [13,14], sublimation of molecular solids [15–17], and binding energies between layered materials [18,19]. In recent years, some attempts [20,21] have been made to develop computationally efficient semilocal density functionals that extend the short-range description, but in general, a long-range van der Waals (vdW) correction is needed. This failure due to the absence of vdW interactions seriously limits the applicability of conventional DFT to a broad class of systems such as molecular solids [22–28] and complexes as well as biological systems [29] in which the long-range vdW interaction plays an important role. A quick remedy for this inadequacy is to develop a vdW correction for the missing long-range part and add it to the DFT part. This combined DFT+vdW approach has become one of the most popular methods in electronic-structure calculations.

In the large-separation ($d \to \infty$) limit, the vdW interaction takes a simple asymptotic expression [30]

$$E_{\rm vdW} = -C_6/d^6 - C_8/d^8 - C_{10}/d^{10} - \cdots , \qquad (1)$$

where d is the distance between centers of density fragments, which may or may not belong to part of the same object. C_6, C_8, and C_{10} are the vdW coefficients, describing dipole-dipole (C_6), dipole-quadrupole (C_8), and dipole-octupole and quadrupole-quadrupole (C_{10}) interactions, respectively. In the development of the vdW correction, there are two important tasks: One is to remove the unphysical divergence when the separation between objects is small, and the other is to calculate vdW coefficients. The first issue can be addressed by properly designing a damping function [31,32] for each asymptotic term [30]. Quite a few well-designed damping functions have been proposed and widely used [31,33,34] in vdW corrections. The second issue involves complicated many-body effects. These effects can be accurately captured with standard wave-function-based many-body methods, such as the time-dependent Hartree-Fock method (TDHF), time-dependent Møller-Plesset second-order perturbation theory (TDMP2), coupled-cluster methods [e.g., coupled-cluster with single, double, and partially triple excitations, CCSD(T)], and random-phase approximation (RPA) methods or their combinations, but these methods are usually limited to small and middle-size molecules due to high computational cost. As such, accurate modeling of vdW coefficients has been highly desired. Many atom-pairwise-based models have been proposed [34–38]. Due to their simplicity and good accuracy, some of them have been widely used in electronic-structure calculations. However, the errors of atom-pairwise-based

*Corresponding author: jianmin.tao@temple.edu; http://www.sas.upenn.edu/∼jianmint/

models are usually size dependent [39] and can be large for nanostructures. This size-dependent error arises from many-body interactions and cannot be solved through a damping function. Although in practical applications it is not necessary to use the absolutely accurate vdW coefficients, it is highly desired to use them. The reason is that absolutely accurate vdW coefficients can reflect the correct many-body effects contained in these coefficients and thus enable us, to a great extent, to reveal the true physics informed by the vdW correction.

In recent years, several methods beyond atom-pairwise-based models for the calculation of vdW coefficients have been developed [40–51]. A common feature of these beyond-atom-pairwise-based methods is that they treat the electrons to be distributed over the whole system, rather than partition them in terms of atoms in a molecule. In other words, the electron density in a whole system is used as input, and therefore, many effects, such as nonadditive many-body interactions and electron delocalization, that are missing in atom-pairwise-based models can be accounted for either implicitly or explicitly by these models. As a result, the error of these models can be nearly size independent. For example, Tkatchenko *et al.* [39] proposed a model dipole polarizability based on a system of coupled quantum harmonic oscillators, which goes beyond the atom-pairwise-based model of Tkatchenko and Scheffler [35]. The former does not show size-dependent error, but the latter does. Recently, we have applied [16] the Rutgers-Chalmers [41] vdW-DF to calculate the sublimation energies of several small fullerenes. We found that the electron-gas-based vdW-DF obtained from the fluctuation-dissipation theorem yields consistently accurate sublimation energies, without suffering size-dependent error. Tao and coworkers [47,49] proposed two molecular-based models, the solid-sphere model and hollow-sphere model. The former was proposed for the calculation of vdW coefficients between atoms and/or molecules, while the latter is more flexible and valid for molecular pairs that may or may not have any cavity. It has been shown that these two models are accurate for nanostructures [52]. Since the inputs to these two models are the accurate static multipole polarizability and the electron density of a whole system, they are multicenter based. (Atom-pairwise-based models are one center based.) As a result, the errors of the two models are nearly size independent, as confirmed by vdW coefficients for nanoclusters [49,50,52]. More recently, one of the present authors [50] applied the solid-sphere model to calculate both the leading-order and higher-order vdW coefficients between small molecules, within the modified single-frequency approximation (see discussion below). The results are in very good agreement with expensive TDMP2 or TDHF calculations, with mean absolute relative errors of 6% for C_6, 5% for C_8, and 7% for C_{10}. This is very encouraging.

Fullerenes are related to nanotubes and graphene. They can be used as a clean energy storage (e.g., hydrogen storage [53]). The high sublimation energies of fullerenes can make them attractive candidates as rapid coolant [54] for astronauts. In this work, we apply the hollow-sphere model in the modified single-frequency approximation to study the vdW coefficients between fullerenes, fullerene and alkali atoms, and fullerene and sodium clusters. We find that the model can generate vdW coefficients C_6 in excellent agreement with highly accurate *ab initio* calculations, with a mean absolute relative error of only 3%. We also show that the nonadditivities of vdW coefficients C_6 between fullerenes and between a fullerene molecule (e.g., C_{60}) and sodium clusters revealed by the model agree very well with the accurate *ab initio* prediction, both of which display oscillating nonadditivity but in opposite trends.

II. HOLLOW-SPHERE MODEL

The starting point of the hollow-sphere model is the classical conducting spherical shell of density that is uniform inside and zero outside the shell. It was constructed to model the dynamic multipole polarizability of a shell of inhomogeneous density that allows for a cavity. The model combines the advantages of the solid-sphere model [46,47] and the classical shell model [48,55] and is equally valid for molecules with and without a cavity. It recovers the classical shell model in the uniform-gas limit with a sharp physical boundary and the solid-sphere model when the cavity of a molecule vanishes. So this unified hollow-sphere model is quite flexible and can be used in different situations to study the vdW interaction (e.g., vdW interaction between fullerenes and atoms or clusters without cavity). The model satisfies the exact zero- and high-frequency limits for each order and takes the simple expression [16,49]

$$\alpha_l(iu) = \frac{2l+1}{4\pi a_l}\int_{R_l-t_l}^{R_l} d^3r\left(\frac{r^{2l-2}a_l^4\omega_l^2}{a_l^4\omega_l^2+u^2}\right)\frac{1}{1-\beta_l\rho_l}, \qquad (2)$$

where iu is the imaginary frequency, R_l is the effective vdW outer radius of the shell, and $R_l - t_l$ is the effective vdW inner radius. $\beta_l(\mathbf{r}) = \omega_l^2(\mathbf{r})\tilde{\omega}_l^2(\mathbf{r})/\{[\omega_l^2(\mathbf{r})+u^2][\tilde{\omega}_l^2(\mathbf{r})+u^2]\}$ describes the coupling of the local sphere and cavity plasmon oscillations, and $\rho_l = (1-t_l/R_l)^{2l+1}$ describes the shape of the shell, with t_l being the shell thickness [49,56]. $\omega_l(\mathbf{r}) = \omega_p(\mathbf{r})\sqrt{l/(2l+1)}$ is the generalized local plasmon frequency of a sphere, $\tilde{\omega}_l(\mathbf{r}) = \omega_p(\mathbf{r})\sqrt{(l+1)/(2l+1)}$ is the generalized local plasmon frequency of a cavity, and $\omega_p(\mathbf{r}) = \sqrt{4\pi n(\mathbf{r})}$ is the local plasmon frequency of the extended electron gas. (Atomic units are used.) The parameters R_l and a_l are determined by the static and high-frequency limits [52], leading to the coupled equations

$$R_l = [a_l\alpha_l(0)]^{1/(2l+1)}, \qquad (3)$$

$$a_l = \left\{\int_0^\infty dr 4\pi r^{2l}n(r)\Big/\int_{R_l-t_l}^{R_l} dr 4\pi r^{2l}n(r)\right\}^{1/3}. \qquad (4)$$

III. SINGLE-FREQUENCY APPROXIMATION

To simplify the calculation, the single-frequency approximation (SFA) was proposed [49], which assumes that only valence electrons are polarizable and that the density is uniform inside the shell and zero otherwise. In the SFA, $d_l = 1$ and the model polarizability of a molecule is simplified as

$$\alpha_l^{\mathrm{SFA}}(iu) = \left(R_l^{2l+1}\frac{\omega_l^2}{\omega_l^2+u^2}\right)\frac{1-\rho_l}{1-\beta_l\rho_l}, \qquad (5)$$

where $R_l = [\alpha_l^{\mathrm{SFA}}(0)]^{1/2l+1}$, with $\alpha_l^{\mathrm{SFA}}(0) = \alpha_l(0)$ being the accurate static multipole polarizability. β_l, the shape function ρ_l, and the plasmon frequency ω_l are defined below Eq. (2), but

with the local electron density replaced by the average valence electron density $\bar{n}$. The average valence electron density can be calculated from $\bar{n} = N/V_l$, where N is the number of valence electrons and V_l is the shell volume given by $V_l = (4\pi/3)[R_l^3 - (R_l - t_l)^3]$. In SFA, the accurate static multipole polarizability $\alpha_l(0)$ is the only required input, which can be calculated from *ab initio* methods such as TDHF or TDMP2 or time-dependent DFT [57] (TDDFT). Compared to the full-frequency calculation required in the wave-function-based many-body calculations [58] of the dynamic polarizability, the single-point-frequency calculation of the static polarizability is much cheaper and very practical for large molecules and nanomaterials. The hollow-sphere model within the SFA is rather similar to the classical shell model. However, there is an important distinction. The former has no sharp physical boundary, while the latter does. The hollow-sphere model is exact in the zero-frequency limit and more correct in the high-frequency limit. As a result, the hollow-sphere model within the SFA is more accurate than the classical shell model.

However, there is an ambiguity in the SFA when we count the number of valence electrons of an atom in a molecule. In previous work [49], the number of valence electrons included all electrons in the outermost shell of an atom. As argued recently by Tao and Rappe [50], valence electrons should only include those in the outermost *subshell* because electrons in the outermost subshell have the greatest probability to appear in valence regions rather than core regions and thus are diffuse and much more easily deformed by external fields or polarized. For example, electrons in the np orbital are much more likely to be deformed by an external electric field than electrons in the ns orbitals. Furthermore, the difference in the shape of ns and np orbitals in an atom leads to the larger deformation of the outermost np valence electrons than ns valence electrons. This counting method has been adopted in the Slater-Kirkwood method [59]. We call this counting method the modified single-frequency approximation (MSFA). Figure 1 shows a comparison of the model dynamic dipole polarizability in the SFA and MSFA to the TDHF calculation. From Fig. 1 we can see that, in the zero-frequency limit, SFA and MSFA are exact. However, in the high-frequency region, only the full hollow-sphere model is exact, suggesting that the full hollow-sphere model has a good chance of being more accurate than MSFA (see Table IV below). This can be understood by regarding the model as an interpolation of imaginary frequency between the zero- and high-frequency limits. Nevertheless, in the important middle range of frequencies, MSFA is closer to the TDHF value than SFA. Therefore, MSFA should be more accurate than SFA. (For alkali atoms, MSFA and SFA are the same.)

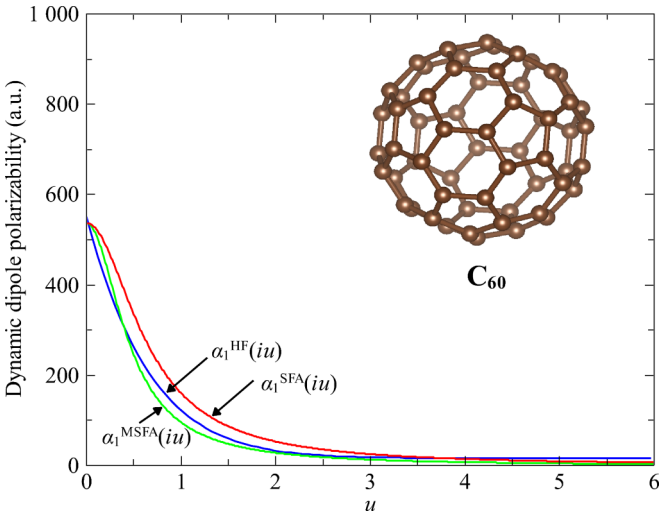

FIG. 1. Comparison of the dynamic dipole polarizability as a function of the imaginary frequency iu of C_{60} evaluated with the hollow-sphere model within the original single-frequency approximation [49] (SFA) and modified SFA (MSFA) to the TDHF value [60].

To have a better understanding of the cavity effect, we apply the solid-sphere model [46,47]

$$\alpha_l(iu) = \frac{2l+1}{4\pi a_l}\int_0^{R_l} d^3r\left(\frac{r^{2l-2}a_l^4\omega_l^2}{a_l^4\omega_l^2+u^2}\right), \tag{6}$$

to study molecules with a cavity. For such molecules, the electron density is zero outside the shell. Thus, we can rewrite Eq. (6) as

$$\alpha_l(iu) = \frac{2l+1}{4\pi a_l}\int_{R_l-t_l}^{R_l} d^3r\left(\frac{r^{2l-2}a_l^4\omega_l^2}{a_l^4\omega_l^2+u^2}\right). \tag{7}$$

From Eqs. (2) and (7), we can see that the solid-sphere model is just the hollow-sphere model in which coupling to the cavity plasmon is dropped. In the static or zero-frequency limit, we obtain [49]

$$\alpha_l(0) = R_l^{2l+1} - (R_l - t_l)^{2l+1}. \tag{8}$$

With the parameter set $l = 1$, $R_1 = 8.703$, and $t_1 = 3.4$, we can easily find $\alpha_l(0) = 510.1$ from Eq. (8), while the TDDFT value is 659.1, as given in Table I. This suggests that the solid-sphere model noticeably underestimates the static polarizability and thus the vdW coefficients. However, if the accurate-input static polarizability employed in the hollow-sphere model is also used in the solid-sphere model of Eq. (6) and we imagine a fullerene or cage molecule as a solid sphere (i.e., $t_l = R_l$), the leading-order vdW coefficient C_6 will increase by only 3% (relative to the prediction of the hollow-sphere model in Table II) for the C_{60}-C_{60} pair and by 4% for C_{84}-C_{84}. For C_{10}, it will increase more (5% for the C_{60}-C_{60} pair and 6% for the C_{84}-C_{84} pair), leading to a mean absolute relative error (MARE) of >6% for the solid-sphere model. Clearly, coupling to the cavity plasmon is important and should be considered in any case for accurate modeling of vdW coefficients between cage molecules.

IV. VDW COEFFICIENTS

The vdW coefficients can be generated with the dynamic multipole polarizability $\alpha_l(iu)$ using the second-order perturbation theory expression or the Casimir-Polder formula [61],

$$C_{2k}^{AB} = \frac{(2k-2)!}{2\pi}\sum_{l_1=1}^{k-2}\frac{1}{(2l_1)!(2l_2)!}\int_0^\infty du\alpha_{l_1}^A(iu)\alpha_{l_2}^B(iu). \tag{9}$$

Within the SFA or MSFA, the sixfold integral in position space is reduced to a two-fold integral, which can be done analytically. This approximation significantly reduces

TABLE I. Input static multipole polarizabilities (in a.u.) of fullerenes, alkali atoms, and sodium clusters.

Atom	N	$\alpha_1(0)$	$\alpha_2(0)$	$\alpha_3(0)$
C_{60}	120	536.6[a]	35434[b]	2339833[b]
C_{70}	140	659.1[a]	49917[b]	3780533[b]
C_{78}	156	748.3[a]	61677[b]	5083663[b]
C_{80}	160	798.8[a]	68770[b]	5920460[b]
C_{82}	164	779.7[a]	66051[b]	5595397[b]
C_{84}	168	806.1[a]	69820[b]	6047476[b]
Li	1	164.1[c]	1424[d]	39688[d]
Na	1	162.6[c]	1878[d]	55518[d]
K	1	290.2[c]	5000[d]	176940[d]
Na_2	2	259.5[e]	10558[b]	429524[b]
Na_4	4	511.5[e]	32715[b]	2092376[b]
Na_6	6	743.9[e]	61074[b]	5014189[b]
Na_8	8	883.9[e]	81409[b]	7497918[b]
Na_{10}	10	1053[e]	108988[b]	11280617[b]
Na_{12}	12	1342[e]	163275[b]	19865029[b]
Na_{14}	14	1652[e]	230861[b]	32261912[b]
Na_{18}	18	1725[e]	248112[b]	35686824[b]
Na_{20}	20	1988[e]	314312[b]	49694107[b]

[a]From [60].
[b]Estimated from the conventional formula $\alpha_l(0) = [\alpha_1(0)]^{(2l+1)/3}$. See text for discussion.
[c]From [62].
[d]From [63].
[e]From [49,64]

the computational cost, which is particularly important for nanostructures. The analytic expression for the integrated vdW coefficients over the frequency can be found in Ref. [52].

Now, we apply the hollow-sphere model in the MSFA to calculate the vdW coefficients for fullerene pairs, for which accurate reference values are available for comparison. In our calculations, we set the thickness $t = 3.4$ bohrs, as suggested in Ref. [56]. The input static dipole polarizabilities of fullerenes are taken from the TDHF calculations [60], while the static higher-order multipole polarizabilities are estimated from the conventional formula $\alpha_l(0) = [\alpha_1(0)]^{(2l+1)/3}$. (For convenience, all the input static polarizabilities are listed in Table I.) For carbon atoms, the number of valence electrons in the outmost subshell is 2. (In previous studies [49], the number of valence electrons is taken to be 4, which includes the electrons in all the outmost subshells with the same principal quantum number). The results are given in Table II. From Table II, we observe that MSFA can yield C_6 consistently, in excellent agreement with the expensive TDHF calculations, with a MARE of only 3%, which significantly improves the accuracy of the original SFA [49]. This accuracy benefits from the fact that the electrons on the surface of fullerenes are nearly uniform due to the full delocalization of π electrons. This can be understood from the low-energy gap of fullerenes. (The largest energy gap of fullerenes is about 2 eV, which occurs for C_{60}.) The good performance of the model on vdW coefficients for fullerene pairs is expected. The more slowly varying the electron density is, the more accurate the model polarizability will be. In the uniform-gas limit, the model becomes exact. In addition, fullerenes also have quasispherical symmetry.

TABLE II. The vdW coefficients C_6, C_8, and C_{10} (in a.u.) for 21 fullerene pairs calculated using the hollow-sphere model (HSM) within the modified SFA (MSFA). The input static dipole polarizabilities of fullerenes are taken from Ref. [60], while the static quadrupole and octupole polarizabilities are estimated from the conventional formula $\alpha_l(0) = [\alpha_1(0)]^{(2l+1)/3}$. The reference values of C_6 are taken from Ref. [60]. MRE = mean relative error. MARE = mean absolute relative error.

	$C_6^{\rm ref}/10^3$	$C_6^{\rm MSFA}/10^3$	$C_8^{\rm MSFA}/10^5$	$C_{10}^{\rm MSFA}/10^7$
C_{60}-C_{60}	100.1	98.91	356.9	1059
C_{60}-C_{70}	119.0	121.5	470.5	1497
C_{60}-C_{78}	133.5	137.9	559.4	1862
C_{60}-C_{80}	138.7	147.2	611.9	2086
C_{60}-C_{82}	140.4	143.7	591.9	2000
C_{60}-C_{84}	144.2	148.6	619.6	2119
C_{70}-C_{70}	141.6	144.7	601.8	2057
C_{70}-C_{78}	158.8	164.3	713.4	2545
C_{70}-C_{80}	165.0	175.4	779.2	2844
C_{70}-C_{82}	166.9	171.2	754.1	2729
C_{70}-C_{84}	171.5	177.0	788.8	2888
C_{78}-C_{78}	178.2	184.2	836.1	3119
C_{78}-C_{80}	185.1	196.6	912.4	3479
C_{78}-C_{82}	187.3	191.9	883.3	3341
C_{78}-C_{84}	192.4	198.4	923.6	3533
C_{80}-C_{80}	192.5	205.4	975.3	3805
C_{80}-C_{82}	194.6	200.5	944.3	3655
C_{80}-C_{84}	199.9	207.3	987.2	3864
C_{82}-C_{82}	196.8	200.7	937.0	3596
C_{82}-C_{84}	202.2	207.5	979.6	3801
C_{84}-C_{84}	207.7	213.3	1019	4002
MRE (%)		3.3		
MARE (%)		3.4		

All these characteristics make fullerenes very suitable for the model.

Next, we apply the model to calculate the vdW coefficients between fullerene C_{60}-alkali atoms and C_{60}-sodium cluster pairs. For atoms and sodium clusters with no cavity, we set the shell thickness to be the conventional vdW radius (i.e., the vdW cutoff radius of a solid sphere), $t_l = [\alpha_l(0)]^{1/(2l+1)}$. For alkali atoms, we take the highly accurate static dipole polarizabilities from Ref. [62] and higher-order multipole polarizabilities from Ref. [63]. For sodium clusters, only the static dipole polarizabilities from *ab initio* calculations are available in the literature. Since the electron density in sodium clusters is much slower than in atoms, to a good approximation, we estimate the static higher-order multipole polarizabilities from the conventional formula $\alpha_l(0) = [\alpha_1(0)]^{3/(2l+1)}$, as given in Table I. Here the number of valence electrons of each atom is only 1 in the *ns* orbital. The results are given in Table III. We observe from Table III that the vdW coefficients generated from the hollow-sphere model consistently agree very well with the reference values, achieving the same MARE of 3% as found for fullerene pairs.

Finally, we apply the hollow-sphere model to study the vdW coefficients between C_{60} and alkali atoms, with and without MSFA. Since the dynamic polarizability of C_{60} within SFA agrees well with the TDHF value within the whole frequency

TABLE III. The vdW coefficients C_6, C_8, and C_{10} (in a.u.) for C_{60}-alkali atom and C_{60}-sodium cluster pairs (no cavity) calculated from the hollow-sphere model within the modified SFA (MSFA). For alkali atoms and sodium clusters, we set $t_l = R_l = [\alpha_l(0)]^{(2l+1)/3}$ and $\rho_l = 0$. The input static multipole polarizabilities of alkali atoms are taken from Refs. [62,63], while the static dipole polarizabilities of sodium clusters are from Ref. [64]. For sodium clusters, the quadrupole and octupole polarizabilities are estimated from the conventional formula $\alpha_l(0) = [\alpha_1(0)]^{(2l+1)/3}$. The reference values of C_6 are taken from Refs. [64,65]. MRE = mean relative error. MARE = mean absolute relative error.

	$C_6^{\rm ref}/10^3$	$C_6^{\rm MSFA}/10^3$	$C_8^{\rm MSFA}/10^5$	$C_{10}^{\rm MSFA}/10^7$
C_{60}-Li	8.07	8.80	17.70	28.85
C_{60}-Na	8.52	8.75	18.28	31.27
C_{60}-K	12.95	12.14	27.66	52.98
C_{60}-Na_2	15.72	15.37	42.97	99.22
C_{60}-Na_4	30.24	30.49	104.4	296.0
C_{60}-Na_6	43.92	44.91	175.8	567.7
C_{60}-Na_8	54.72	55.99	234.2	806.4
C_{60}-Na_{10}	66.60	68.03	305.5	1125
C_{60}-Na_{12}	82.08	84.58	421.1	1709
C_{60}-Na_{14}	98.28	101.8	556.6	2464
C_{60}-Na_{18}	113.4	115.8	645.9	2914
C_{60}-Na_{20}	127.2	131.5	783.9	3762
MRE (%)		1.9		
MARE (%)		3.3		

range, as shown by Fig. 1, in this study, we use $\alpha_l^{\rm MSFA}(iu)$ of Eq. (5) for C_{60} while the dynamic multipole polarizability of atoms ($t_l = R_l$) with and without MSFA is used. The results are given in Table IV. From Table IV, we observe that the vdW coefficients generated with the full hollow-sphere model (i.e., without MSFA) are more accurate than those with MSFA.

V. NONADDITIVITY OF C_6

Despite considerable progress in the development of vdW corrections, calculation of vdW coefficients between nanostructures remains a difficult task due to the nonadditivity. Nonadditivity of the vdW interaction has been an important issue that hinders the development of universally accurate vdW corrections. Many efforts have been made to understand this problem [39,48,49,60,66–68]. This is particularly important for molecules with full valence electron delocalization, such as metallic systems (e.g., alkali clusters) and conjugated molecules, in which vdW coefficients display very strong

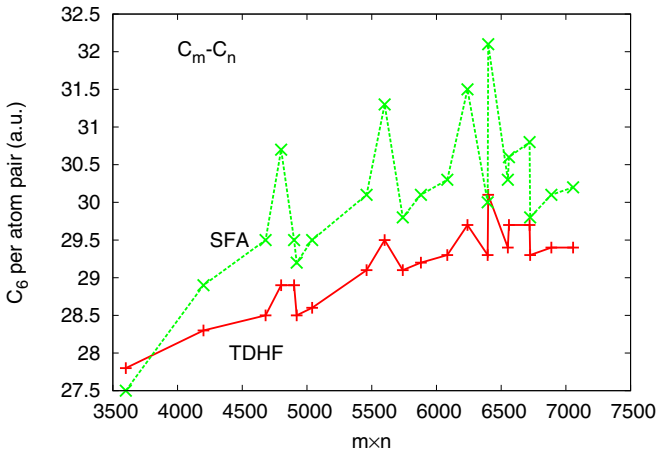

FIG. 2. Variation of the vdW coefficient C_6 per carbon atom pair for fullerene pairs vs the number of carbon atom pairs formed between fullerene molecules.

nonadditivity. In this work, we study the nonadditivity of the vdW coefficients between small fullerene molecules and fullerene C_{60} and sodium clusters Na_n.

Figure 2 shows that C_6 per carbon atom is oscillatingly increasing for fullerene pairs. This suggests that the error of simple atom-pairwise-based models grows with system size for molecular pairs involving fullerenes. The nonadditivity of C_6 between fullerene pairs including identical as well as nonidentical pairs is quite different from that of C_6 between only identical pairs, the latter of which was found to be monotonically increasing [48,49,60]. Interestingly, we find that C_6 per sodium atom decreases with the increase of the number of sodium atoms between a fullerene and sodium clusters, as shown in Fig. 3. A similar trend was observed for identical sodium cluster pairs [49,52], but the decreasing rate between fullerene and sodium clusters is slower than that between identical sodium clusters. In both cases, the trends revealed by our model agree well with those displayed by TDHF [60,64].

VI. CONCLUSION

In summary, we have applied the hollow-sphere model within the MSFA to the calculation of the vdW coefficients between fullerenes, fullerene and alkali atoms, and fullerene and sodium clusters. The results are in excellent agreement with the expensive TDHF calculations, with an overall MARE of only 3%. Compared to the original SFA, the MSFA yields

TABLE IV. The vdW coefficients C_6, C_8, and C_{10} (in a.u.) between C_{60} and alkali atoms calculated from the hollow-sphere or solid-sphere model with and without the modified SFA (MSFA) for alkali atoms while the dynamic polarizability of C_{60} of Eq. (5) is used. For atoms, $t_l = R_l$ (no cavity). FHSM = full hollow-sphere model of Eq. (7). MRE = mean relative error. MARE = mean absolute relative error.

	$C_6^{\rm ref}/10^3$	$C_6^{\rm FHSM}/10^3$	$C_6^{\rm MSFA}/10^3$	$C_8^{\rm FHSM}/10^5$	$C_8^{\rm MSFA}/10^5$	$C_{10}^{\rm FHSM}/10^7$	$C_{10}^{\rm MSFA}/10^7$
C_{60}-Li	8.07	8.19	8.80	17.14	17.70	29.72	28.85
C_{60}-Na	8.52	8.86	8.75	18.96	18.28	33.83	31.27
C_{60}-K	12.95	13.93	12.14	31.84	27.66	62.71	52.98
MRE (%)		4.4	1.8				
MARE (%)		4.4	6.0				

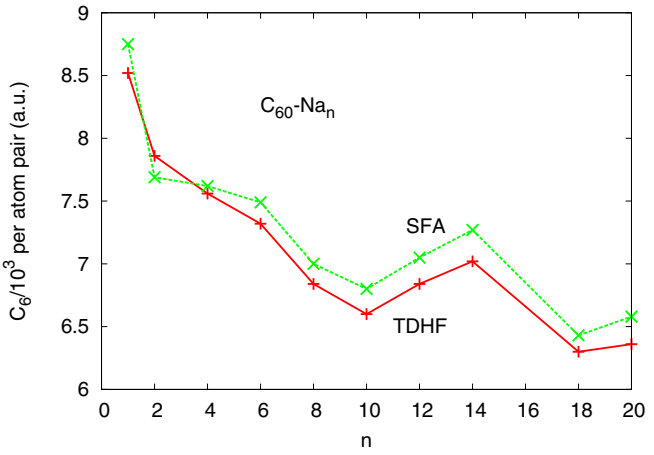

FIG. 3. Variation of the vdW coefficient $C_6/10^3$ per sodium atom pair between C_{60} and sodium clusters vs the number of sodium atoms in sodium clusters.

the dynamic dipole polarizability in better agreement with the TDHF values for fullerene C_{60}, in particular in the important low-frequency region. This accuracy is consistent with a recent application to diatomics and small molecules [50], where it was found that the MSFA yields accurate vdW coefficients, with a MARE of 6% for C_6, 5% for C_8, and 7% for C_{10}. This small relative error difference is largely due to the fact that the electron density on the surface of fullerenes and in sodium clusters is not rapidly varying, but it is for small molecules, in particular diatomics. Another difference between fullerenes and sodium clusters and small molecules is that the former have higher symmetry. But this geometrical effect is relatively small, compared to the spatial variation of the electron density. This can be seen from the vdW coefficients involving atoms calculated within the MSFA in Refs. [50,52] and this work (Table III). Atomic densities are of spherical symmetry, but they are rapidly varying. However, the error of the vdW coefficients involving atoms is larger than those with lower symmetry but slower spatial variation of the electron density, such as molecules, suggesting that the spatial variation of the density is more important than the symmetry of the system, making the model particularly attractive for intermolecular applications. As such, the hollow-sphere model seems to provide a promising way to accurately treat the vdW coefficients.

Since the surface electrons of fullerenes are fully nonlocal and thus display strong nonadditivity [48,49,60], as further demonstrated in this work, this model will play an important role in the simulation of vdW corrections/interactions involving fullerenes, such as adsorption of fullerenes on metal surfaces as well as atoms and molecules on the surface of fullerenes. Because the model is valid for all thicknesses t, including ending points, it is also valid for molecules without a cavity [50]. Therefore, it can also be used to simulate vdW interactions between molecules, regardless of whether there is any cavity or not. This flexibility allows us to treat different situations on the same footing. Taking the simplification one step further without knowledge of the true electron density should be very useful for large nanostructures.

In addition, our model may serve as a starting point for a better fundamental understanding of nanostructures such as nanotubes, graphene, and other vdW layered materials and complexes. In particular, it can be used to investigate the nonadditivity of vdW coefficients due to its very good accuracy, size-independent error, and flexibility.

ACKNOWLEDGMENTS

We thank Haowei Peng and Zeng-Hui Yang for helpful comments and suggestions. J.T. and Y.M. acknowledge support from the NSF under Grant No. CHE 1640584. G.T. was supported by the China Scholarship Council and the National Natural Science Foundation of China under Grant No. 51264021.

[1] J. P. Perdew, K. Burke, and M. Ernzerhof, Phys. Rev. Lett. **77**, 3865 (1996).
[2] J. Tao, J. P. Perdew, V. N. Staroverov, and G. E. Scuseria, Phys. Rev. Lett. **91**, 146401 (2003).
[3] J. P. Perdew, A. Ruzsinszky, J. Tao, V. N. Staroverov, G. E. Scuseria, and G. I. Csonka, J. Chem. Phys. **123**, 062201 (2005).
[4] J. Tao and J. P. Perdew, J. Chem. Phys. **122**, 114102 (2005).
[5] A. D. Becke, J. Chem. Phys. **104**, 1040 (1996).
[6] A. D. Becke, Phys. Rev. A **38**, 3098 (1988).
[7] C. Lee, W. Yang, and R. G. Parr, Phys. Rev. B **37**, 785 (1988).
[8] Y. Zhao and D. G. Truhlar, J. Chem. Phys. **125**, 194101 (2006).
[9] J. Heyd, G. E. Scuseria, and M. Ernzerhof, J. Chem. Phys. **118**, 8207 (2003).
[10] J. P. Perdew, A. Ruzsinszky, G. I. Csonka, O. A. Vydrov, G. E. Scuseria, L. A. Constantin, X. Zhou, and K. Burke, Phys. Rev. Lett. **100**, 136406 (2008).
[11] V. N. Staroverov, G. E. Scuseria, J. Tao, and J. P. Perdew, J. Chem. Phys. **119**, 12129 (2003); **121**, 11507(E) (2004).
[12] V. N. Staroverov, G. E. Scuseria, J. Tao, and J. P. Perdew, Phys. Rev. B **69**, 075102 (2004).
[13] J. Tao and A. M. Rappe, Phys. Rev. Lett. **112**, 106101 (2014).
[14] J. Carrasco, W. Liu, A. Michaelides, and A. Tkatchenko, J. Chem. Phys. **140**, 084704 (2014).
[15] K. Berland, O. Borck, and P. Hyldgaard, Comput. Phys. Commun. **182**, 1800 (2011).
[16] J. Tao, J. Yang, and A. M. Rappe, J. Chem. Phys. **142**, 164302 (2015).
[17] P. Hao, J. Sun, B. Xiao, A. Ruzsinszky, G. I. Csonka, J. Tao, S. Glindmeyer, and J. P. Perdew, J. Chem. Theory Comput. **9**, 355 (2013).
[18] L. A. Girifalco and M. Hodak, Phys. Rev. B **65**, 125404 (2002).
[19] B. Sachs, T. O. Wehling, M. I. Katsnelson, and A. I. Lichtenstein, Phys. Rev. B **84**, 195414 (2011).
[20] J. Sun, A. Ruzsinszky, and J. P. Perdew, Phys. Rev. Lett. **115**, 036402 (2015).
[21] J. Tao and Y. Mo, Phys. Rev. Lett. **117**, 073001 (2016).

[22] W. A. Al-Saidi, V. K. Voora, and K. D. Jordan, J. Chem. Theory Comput. **8**, 1503 (2012).
[23] D. A. Egger and L. Kronik, J. Phys. Chem. Lett. **5**, 2728 (2014).
[24] O. Hod, J. Chem. Theory Comput. **8**, 1360 (2012).
[25] A. Otero-de-la-Roza and E. R. Johnson, J. Chem. Phys. **137**, 054103 (2012).
[26] T. Risthaus and S. Grimme, J. Chem. Theory Comput. **9**, 1580 (2013).
[27] J. G. Brandenburg and S. Grimme, Top Curr. Chem. **345**, 1 (2014).
[28] A. Otero-de-la-Roza and E. R. Johnson, J. Chem. Theory Comput. **11**, 4033 (2015).
[29] R. A. DiStasio, O. A. von Lilienfeld, and A. Tkatchenko, Proc. Natl. Acad. Sci. USA **109**, 14791 (2012).
[30] A. Dalgarno and G. A. Victor, Proc. Phys. Soc. **90**, 605 (1967).
[31] Q. Wu and W. Yang, J. Chem. Phys. **116**, 515 (2002).
[32] S. Grimme, S. Ehrlich, and L. Goerigk, J. Comput. Chem. **32**, 1456 (2011).
[33] E. R. Johnson and A. D. Becke, J. Chem. Phys. **124**, 174104 (2006).
[34] S. Grimme, J. Antony, S. Ehrlich, and H. Krieg, J. Chem. Phys. **132**, 154104 (2010).
[35] A. Tkatchenko and M. Scheffler, Phys. Rev. Lett. **102**, 073005 (2009).
[36] A. D. Becke and E. R. Johnson, J. Chem. Phys. **127**, 154108 (2007).
[37] S. N. Steinmann and C. Corminboeuf, J. Chem. Phys. **134**, 044117 (2011).
[38] S. N. Steinmann and C. Corminboeuf, J. Chem. Theory Comput. **7**, 3567 (2011).
[39] A. Tkatchenko, R. A. DiStasio, R. Car, and M. Scheffler, Phys. Rev. Lett. **108**, 236402 (2012).
[40] E. Hult, H. Rydberg, B. I. Lundqvist, and D. C. Langreth, Phys. Rev. B **59**, 4708 (1999).
[41] M. Dion, H. Rydberg, E. Schröder, D. C. Langreth, and B. I. Lundqvist, Phys. Rev. Lett. **92**, 246401 (2004).
[42] P. Hyldgaard, K. Berland, and E. Schröder, Phys. Rev. B **90**, 075148 (2014).
[43] K. Berland, V. R. Cooper, K. Lee, E. Schröder, T. Thonhauser, P. Hyldgaard, and B. I. Lundqvist, Rep. Prog. Phys. **78**, 066501 (2015).
[44] O. A. Vydrov and T. Van Voorhis, J. Chem. Phys. **133**, 244103 (2010).
[45] R. Sabatini, T. Gorni, and S. de Gironcoli, Phys. Rev. B **87**, 041108(R) (2013).
[46] J. Tao, J. P. Perdew, and A. Ruzsinszky, Phys. Rev. B **81**, 233102 (2010).
[47] J. Tao, J. P. Perdew, and A. Ruzsinszky, Proc. Natl. Acad. Sci. **109**, 18 (2012).
[48] A. Ruzsinszky, J. P. Perdew, J. Tao, G. I. Csonka, and J. M. Pitarke, Phys. Rev. Lett. **109**, 233203 (2012).
[49] J. Tao and J. P. Perdew, J. Chem. Phys. **141**, 141101 (2014).
[50] J. Tao and A. M. Rappe, J. Chem. Phys. **144**, 031102 (2016).
[51] J. Tao, J. P. Perdew, and A. Ruzsinszky, Int. J. Mod. Phys. B **27**, 1330011 (2013).
[52] J. Tao, Y. Fang, P. Hao, G. E. Scuseria, A. Ruzsinszky, and J. P. Perdew, J. Chem. Phys. **142**, 024312 (2015).
[53] T. T. Vehviläinen, M. G. Ganchenkova, L. E. Oikkonen, and R. M. Nieminen, Phys. Rev. B **84**, 085447 (2011).
[54] M. S. Dresselhaus, G. Dresselhaus, and P. C. Eklund, *Science of Fullerenes and Carbon Nanotubes* (Academic, London, 1995).
[55] J. P. Perdew, J. Tao, P. Hao, A. Ruzsinszky, G. I. Csonka, and J. M. Pitarke, J. Phys. Condens. Matter **24**, 424207 (2012).
[56] G. K. Gueorguiev, J. M. Pacheco, and D. Tománek, Phys. Rev. Lett. **92**, 215501 (2004).
[57] S. J. A. van Gisbergen, V. P. Osinga, O. V. Gritsenko, R. van Leeuwen, J. G. Snijders, and E. J. Baerends, J. Chem. Phys. **105**, 3142 (1996).
[58] A. Derevianko, S. G. Porsev, and J. F. Babb, At. Data Nucl. Data Tables **96**, 323 (2010).
[59] E. A. Mason and L. Monchick, Adv. Chem. Phys. **12**, 329 (1967).
[60] J. Kauczor, P. Norman, and W. A. Saidi, J. Chem. Phys. **138**, 114107 (2013).
[61] S. H. Patil and K. T. Tang, J. Chem. Phys. **106**, 2298 (1997).
[62] A. Derevianko, W. R. Johnson, M. S. Safronova, and J. F. Babb, Phys. Rev. Lett. **82**, 3589 (1999).
[63] M. Marinescu, H. R. Sadeghpour, and A. Dalgarno, Phys. Rev. A **49**, 982 (1994).
[64] A. Jiemchooroj, P. Norman, and B. E. Sernelius, J. Chem. Phys. **125**, 124306 (2006).
[65] A. Banerjee, J. Autschbach, and A. Chakrabarti, Phys. Rev. A **78**, 032704 (2008).
[66] V. V. Gobre and A. Tkatchenko, Nat. Commun. **4**, 2341 (2013).
[67] R.-F. Liu, J. G. Ángyán, and J. F. Dobson, J. Chem. Phys. **134**, 114106 (2011).
[68] J. F. Dobson, Int. J. Quantum Chem. **114**, 1157 (2014).